Journal of Hazardous Materials 185 (2011) 315–321

Contents lists available at ScienceDirect

Journal of Hazardous Materials

journal homepage: www.elsevier.com/locate/jhazmat

Degradation of C.I. Reactive Red 2 through photocatalysis coupled with water jet cavitation

Xiaoning Wang, Jinping Jia*, Yalin Wang

School of Environmental Science and Engineering, Shanghai Jiao Tong University, Shanghai 200240, PR China

ARTICLE INFO

Article history:
Received 28 June 2010
Received in revised form 7 September 2010
Accepted 7 September 2010
Available online 17 September 2010

Keywords:
Dye
Jet cavitation
Photocatalysis
Synergetic effect
Degradation

ABSTRACT

The decolorization of an azo dye, C.I. Reactive Red 2 was investigated using TiO_2 photocatalysis coupled with water jet cavitation. Experiments were performed in a 4.0 L solution under ultraviolet power of 9 W. The effects of TiO_2 loading, initial dye concentration, solution pH, geometry of cavitation tube, and the addition of anions on the degradation of the dye were evaluated. Degradation of the dye followed a pseudo-first order reaction. The photocatalysis coupled with water jet cavitation elevated degradation of the dye by about 136%, showing a synergistic effect compared to the individual photocatalysis and water jet cavitation. The enhancement of photocatalysis by water jet cavitation could be due to the deagglomeration of catalyst particles as well as the better contact between the catalyst surfaces and the reactants. Venturi tube with smaller diameter and shorter length of throat tube favored the dye decolorization. The degradation efficiency was found to increase with decreasing initial concentration and pH. The presence of NO_3^- and SO_4^{2-} enhanced the degradation of RR2, while Cl^-, and especially HCO_3^- significantly reduced dye decolorization. The results of this study indicated that the coupled photocatalysis and water jet cavitation is effective in degrading dye in wastewater and provides a promising alternative for treatment of dye wastewater at a large scale.

1. Introduction

Dyes constitute a major class of organic compounds, which have a multitude of applications in a variety of industries of textile, paper and leather [1]. It is estimated that more than 15% of the world dye production, about 400 ton per day, are released into the environment during synthesis, processing, and use [2]. Dye-containing wastewaters often receive the great attention due to their strong color that render them visible even at very low concentrations, thus causing serious aesthetic and pollution problems to the water environment [3].

Conventional waste water treatment methods such as flocculation, air sparging, activated carbon adsorption and biological treatment are relatively ineffective in decolorizing dye wastewater, because dyes are generally designed to exhibit high resistance to fading caused by chemical, biological and light-induced oxidation [4]. Moreover, many of the treatment methods merely transfer the dye compounds from water to another phase. Therefore, there is a need for an alternative technology for treating dye-contaminated industrial wastewater. Advanced oxidation processes (AOPs) based on generation of the hydroxyl radical (•OH), an extremely powerful and non-selective oxidizing agent, provide a promising treatment for decolorization [5,6]. Among the various AOPs, photocatalytic oxidation mediated by titanium dioxide in suspension is receiving a great attention [7]. However, UV irradiation is affected by mass transfer limitation and by reduced efficiency of photocatalyst with continuous operation possibly due to the adsorption of contaminants at the surface [8], which obviously limit the practical application of photocatalytic oxidation in real wastewater treatment.

To improve the light utilization efficiency of suspended TiO_2, many attempts [9–11] were taken to introduce ultrasound into photocatalytic reaction system for enhancing the degradation of organic contaminants. This effect is due to the phenomenon of cavitation produced by ultrasound power. Cavitation involves the nucleation, growth and implosive collapse of micro-bubbles or cavities occurring in fractions of microseconds and releasing large quantities of energy over a small location. Thus, cavitation serves as a mean of concentrating the diffuse energy of sound into tiny hot spots that behave as micro-reactor. At the extreme conditions generated inside the cavitation bubbles during collapse, water is thermally dissociated leading to the formation of hydroxyl radicals, which can oxidize organic pollutants in wastewaters [12,13]. Cavitation also has high-energy physical effects, including the improvement of mass transfer, the fragmentation of friable solids and the refreshment of solid surface [13]. However, industrial

* Corresponding author. Tel.: +86 21 54741065; fax: +86 21 54740825.
E-mail address: jpjia@sjtu.edu.cn (J. Jia).

0304-3894/$ – see front matter © 2010 Elsevier B.V. All rights reserved.
doi:10.1016/j.jhazmat.2010.09.036

application of ultrasonically induced cavitation is a problem due to ineffective distribution of the cavitational activity on a large scale and inefficient transfer of electric power into the liquid [14].

An alternative form of cavitation generated by throttling the liquid flow through a constriction, termed hydrodynamic cavitation, has been reported to be more energy efficient than acoustic cavitation. Scale up of hydrodynamic cavitation equipment is relatively easy and maintenance of it is low as compared to those of acoustic cavitation equipment [15,16]. So, it is promising to replace acoustic cavitation with hydrodynamic cavitation in wastewater treatment. Chakinala et al. [17] reported that the use of hydrodynamic cavitation induced by a liquid whistle reactor could enhance the efficacy of the advanced Fenton process by increasing the mass transfer rates, keeping the iron surface active and providing additional free radicals for oxidation. Our earlier work [18] showed that the presence of hydrodynamic cavitation intensifies the electrolysis process by decreasing the diffusion layer thickness on the electrode surface, and consequently increasing the current density. However, the application of hydrodynamic cavitation on photocatalytic reaction has not been reported.

In this study, a large volume of 4.0 L synthetic azo dye solution was used and subjected to photocatalysis in the presence of hydrodynamic cavitation within a venturi tube, herein referred as water jet cavitation. The overall objective is to determine possible enhancement of decolorization of the dye induced by photocatalysis coupled with hydrodynamic cavitation at a larger scale. Photocatalysis combined with mechanical stirring was included for comparison. In addition, some parameters such as TiO_2 dosage, RR2 initial concentration, solution pH, geometry of cavitation tube, and the addition of anions were also investigated.

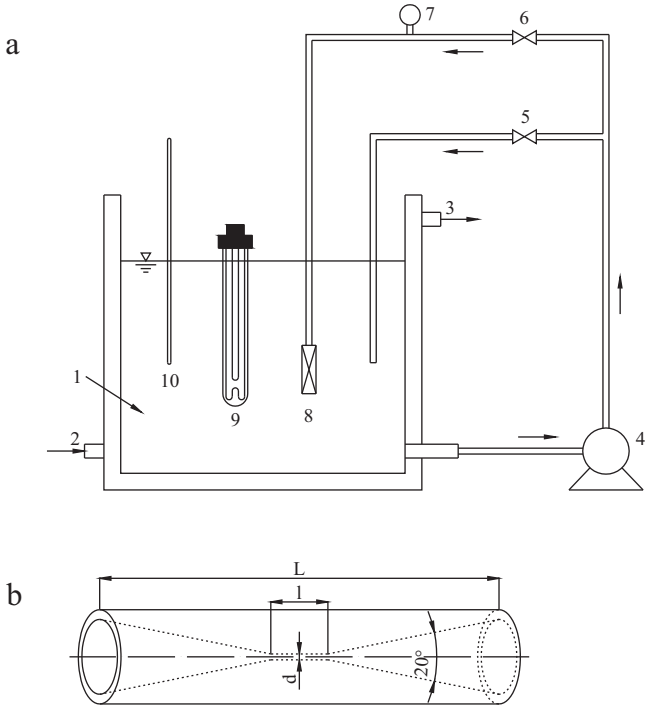

Fig. 1. (a) Experimental setup employed for water jet cavitation, photolysis, photocatalysis, and combination experiments. The pump and lamp were turned on as needed to conduct the individual experiment: 1, tank; 2, inlet of cooling water; 3, outlet of cooling water; 4, self-priming stainless steel pump; 5 and 6, control valves; 7, pressure gauge; 8, cavitation tube; 9, UV lamp; 10, thermometer. (b) Geometry of the cavitation tube: *L*, length of cavitation tube; *l*, length of throat tube; *d*, inner diameter of throat tube.

2. Materials and methods

2.1. Materials

C.I. Reactive Red 2 (RR2) was purchased from Shanghai Jiaying Chemical Co. Ltd. (Shanghai, China) and used as received. Degussa P25 titanium dioxide (80% anatase, 20% rutile, surface area 50 m^2/g) was obtained from Degussa and employed as photocatalyst. H_2SO_4 and NaOH were used to control solution pH. $NaNO_3$, Na_2SO_4, NaCl and $NaHCO_3$ were selected to determine the influence of anions on the decolorization of RR2. All reagents were of analytical grade and used as purchased. Aqueous solutions were prepared using double-distilled water.

2.2. Reactor

The experimental setup (Fig. 1) consisted of a jacketed cylindrical glass reactor (capacity 5000 mL), a UV lamp and a source of jet cavitation. The temperature of the solution was maintained at $30 \pm 3\,^{\circ}C$ by a continuous recirculation of cooling water through the surrounding water jacket. The light source was a 9 W mercury lamp (Shanghai Rongbo Lighting Electrical Appliances Co., Ltd., Shanghai, China) placed inside a quartz tube of 30 mm i.d. and 160 mm height. It was vertically immersed inside the reaction mixture, and emits predominantly at 254 nm wavelength.

The jet flow loop (Fig. 1a) was driven by a high-pressure, self-priming stainless steel pump (Model 25FDB-65D, Shanghai Qiquan Pump Co., Ltd., China) with unidirectional piston and a motor with an electric power of 0.75 kW with a speed of 2900 rpm. The suction side of the pump is connected to the bottom of the holding tank. The discharge from the pump branches into the bypass and main lines. The bypass line has throttling valve (5) for adjusting the pressure and flow rate into the main line. A pressure gauge (7) is provided in the main line to measure the pressure. A venturi tube (Fig. 1b) acts as cavitation part and is equipped at the termination of the main line. Both the bypass line and the main line are dipped into the solution. The inside diameter of the delivery line of the closed loop system is 15 mm. The venturi tube is made of organic glass for visual observation of the movement of the fluid. The expansion angle and contraction angle of the venturi tube are both 20°. The length of venturi tube (*L*), length of throat tube (*l*) and inner diameter of throat tube (*d*) are varied for different venturi tube used. The distance of between UV lamp (9) and venturi tube (8) was fixed at 8 cm.

High inlet pressure and high flow rate through the cavitation tube can improve cavitational activity [19,20]. So, control valve (6) was left open and valve (5) was totally closed in the present work, and thus the highest pressure of 0.34 MP and highest flow rate of 105.7 mL/s were obtained in the mainline. In the separate processes of photolysis and photocatalysis, mechanical stirring was utilized to improve the mass transfer in solution.

2.3. Procedure

All experiments were performed in 4.0 L RR2 solution with reaction time of 90 min. The initial concentration of RR2 was 80 mg/L, TiO_2 dose was 100 mg/L and initial pH was natural 6.7 if not specifically mentioned. To optimize the cavitation part for decolorization of RR2, three venturi tubes of different geometries were used in this study: Tube 1: $L = 128$ mm, $l = 0$ mm and $d = 2$ mm; Tube 2: $L = 123$ mm, $l = 0$ mm and $d = 3$ mm; and Tube 3: $L = 143$ mm, $l = 18$ mm and $d = 3$ mm. Prior to the degradation experiments, suspensions were mechanically stirred for 30 min in the dark to achieve adsorption-desorption equilibrium. For all the conditions investigated, the amount of RR2 adsorbed onto TiO_2 was always less than 5%.

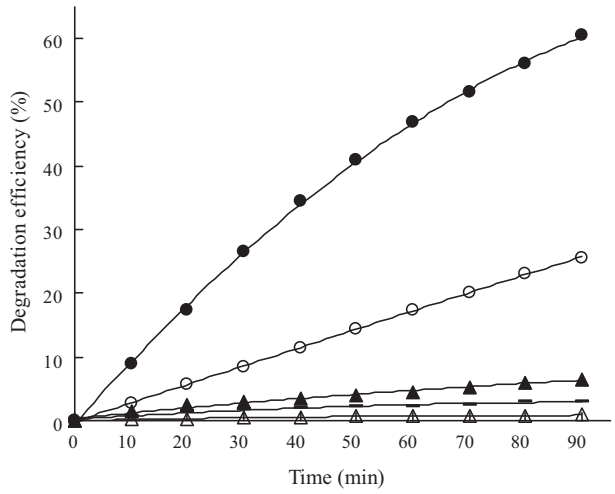

Fig. 2. Degradation of 4.0 L solution containing 80 mg/L RR2 following 90 min of (-—-) water jet cavitation only, (-△-) photolysis under mechanical stirring, (-▲-) simultaneous photolysis and water jet cavitation, (-○-) photocatalysis under mechanical stirring, 100 mg/L TiO_2, and (-●-) simultaneous photocatalysis and water jet cavitation, 100 mg/L TiO_2.

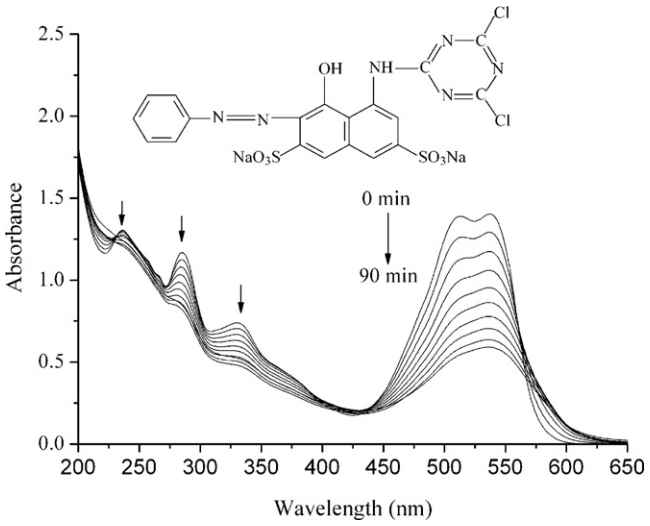

Fig. 3. Temporal variation of UV–vis spectra of an aqueous solution of RR2 recorded following simultaneous photocatalysis and water jet cavitation (initial pH was 6.7; initial RR2 concentration was 80 mg/L; TiO_2 loading was 100 mg/L; Tube 1 was used as cavitation tube; no matrix component was added). Inset shows the chemical structure of RR2.

Samples of the dye solutions were periodically withdrawn from the reaction vessel during all experiments. Solutions were filtered using Millipore 0.45 μm filters to remove the TiO_2 particles. Degradation of the resulting dye solutions was monitored using a Unico UV–vis spectrophotometer (UV-2102 PCS, UNICO, Shanghai). The absorbance was measured at 538 nm which is the characteristic absorption wavelength (λ_{max}) for the RR2 solution. Concentrated dye solutions were diluted prior to measurement to bring the absorbance into the linear range. Percentage of the dye degradation was calculated as % degradation efficiency = $(A_0 - A)/A_0 \times 100\%$, where A_0 and A were initial and measured absorbance of the dye solution. The surface physical morphology of TiO_2 was observed by a scanning electron microscopy (SEM) (S-2150, Hitachi High-Technologies Corp., Japan). The pH value was measured with a PHS-3C pH meter (Shanghai Leici Apparatus Manufactory, Shanghai, China).

3. Results and discussion

3.1. Degradation of dye under different treatment conditions

The degradation of RR2 with treatments of water jet cavitation alone, photolysis under mechanical stirring, photocatalysis under mechanical stirring, photolysis coupled with water jet cavitation, and photocatalysis coupled with water jet cavitation are presented in Fig. 2. The dye was stable with photolysis under mechanical stirring, showing little degradation (0.9%). Although hydrodynamic cavitation generates •OH and other radical species which are capable of attacking organic compounds in solution [20], limited degradation (about 3.1%) of RR2 still occurred within 90 min in the case of water jet cavitation only. When photolysis was combined with water jet cavitation, degradation of RR2 was increased, but no significant enhancement was observed (only 6.5%).

In the presence of TiO_2 particles, the photocatalysis improved degradation of RR2, with up to 25.6% of RR2 being decolorized after 90 min. Moreover, the degradation efficiency was increased sharply to 60.5% when employing UV and jet cavitation simultaneously. This means that the photocatalytic degradation of the dye with water jet cavitation was elevated by about 136%, showing a synergistic effect compared to the individual photocatalysis and water jet cavitation. The major reason for the synergistic effect could be the ability of water jet cavitation to constantly deagglomerate catalyst particles and refresh their surface due to the action of shear stress and micro-streaming generated by cavitation, thereby increasing the overall surface area of catalyst and hence the photoactivity [11]. Moreover, water jet cavitation generates extra hydroxyl radicals, which can also aid the photocatalytic degradation process [21].

The absorption spectra of RR2 solution recorded at time intervals of 10 min following simultaneous photocatalysis and water jet cavitation are shown in Fig. 3. RR2 has four characteristic bands in the UV–vis spectra: one at the visible band (513 and 538 nm) corresponding to the whole conjugated structure connected by azo group; the other three at 331, 285 and 235 nm in the ultraviolet region resulting from the unsaturated structure of naphthalene, triazine and benzene rings, respectively [18,22]. All four absorption bands were decreased with increasing time, indicating the azo bond of the dye molecule was ruptured and the naphthalene, triazine and benzene rings were destroyed during the combined process.

3.2. Effect of geometry of cavitation tube

It has been found that geometry of orifice plate which is a constriction device equipped in hydrodynamic cavitation reactor affects decomposition of compounds and the global reaction rates [23,24]. Hence, it is expected that the geometry of venturi tube, another type of constriction device, would be an important factor for wastewater treatment.

Our experiment shows that the extent of RR2 degradation is affected by both inner diameter of throat tube (d) and length of the throat tube (l) in venturi tube (Fig. 4). The RR2 degradation efficiency decreased from 60.5 to 53.5% at 90 min as the diameter of throat tube increased from 2 mm (Tube 1) to 3 mm (Tube 2). It is possible that smaller diameter decreases the flow area, increases the throat velocity, and in turn increases the cavitational activity, which may enhance photocatalytic process [25]. When length of the throat tube increased from 0 mm (Tube 2) to 18 mm (Tube 3), the RR2 degradation reduced from 53.5% to 47.5%. The observation can be explained that the larger length of throat tube in Tube 3 produces larger levels of power dissipation when the liquid passes through the throat tube, which may reduce the cavitational activity and consequently decreases the RR2 degradation.

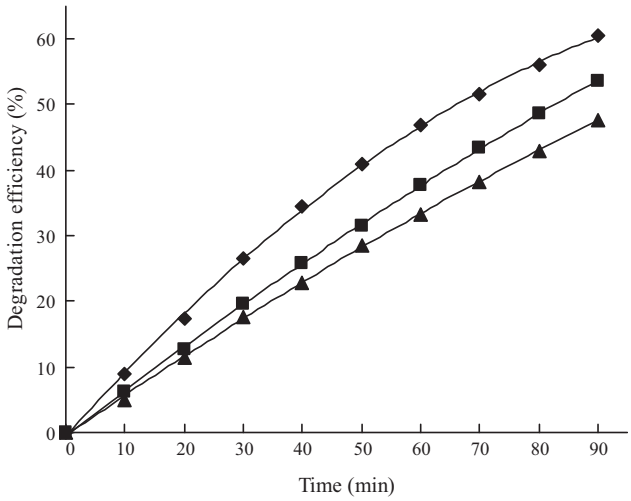

Fig. 4. Effect of geometry of cavitation tube on RR2 degradation during photocatalysis combined with water jet cavitation (initial pH was 6.7; initial RR2 concentration was 80 mg/L; TiO_2 loading was 100 mg/L; no matrix component was added). -♦-, Tube 1: L = 128 mm, l = 0 mm and d = 2 mm; -■-, Tube 2: L = 123 mm, l = 0 mm and d = 3 mm; -▲-, Tube 3: L = 143 mm, l = 18 mm and d = 3 mm.

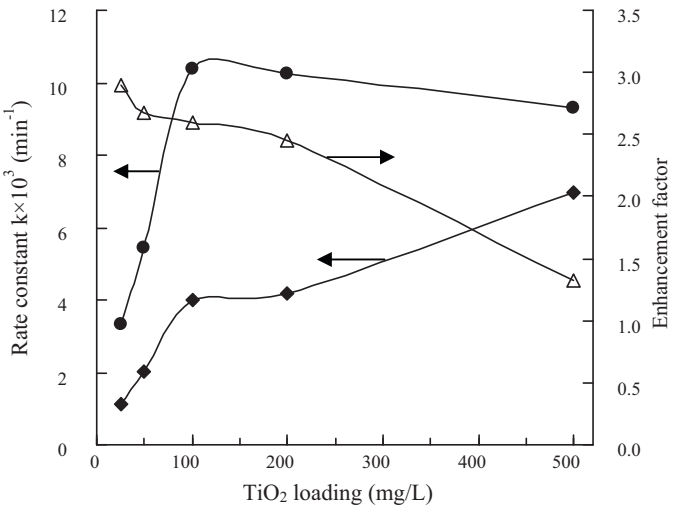

Fig. 5. Effect of TiO_2 loading on the pseudo-first-order rate constants in photocatalysis with water jet cavitation (●) and with mechanical stirring (♦) (initial pH was 6.7; RR2 concentration was 80 mg/L; Tube 1 was used as cavitation tube; no matrix component was added; treatment time was 90 min). Enhancement factor (△) was the ratio of ● to ♦ at the same TiO_2 loading.

3.3. Effect of TiO_2 loading

The variations of the degradation rate constants with different initial TiO_2 loading are shown in Fig. 5. All degradation processes were well described by the pseudo-first-order kinetics. The rate constant of photocatalysis with mechanical stirring increased gradually from 1.14×10^{-3} to 6.97×10^{-3} min^{-1} with TiO_2 loading increasing from 25 to 500 mg/L. This is because the suspensions containing higher amounts of TiO_2 allowed for more fraction of incident light absorbed by the catalysts, leading to a progressively higher production of reactive species on the catalyst surface [26]. When the photocatalysis was coupled with water jet cavitation, the rate constant increased with the increase in the catalyst concentration up to an optimal value of 100 mg/L, followed by a marked decrease. This observation is consistent with some previous literatures [27,28]. In the lower concentration (<100 mg/L) of the catalyst, mass transport of chemical species between the solution phase and the photocatalyst surface may be accelerated, and the photocatalyst surface kept continuous cleaning by water jet cavitation which might increase the amount of reactant to the surface and promote photocatalytic activity of TiO_2. When concentration of catalyst is elevated at more than 100 mg/L, the zone of action of light becomes low due to screening effect of excess TiO_2 particles [29]. As a result, the zone of synergistic action of photocatalysis and water jet cavitation was limited.

However, the photocatalysis coupled with water jet cavitation improved the rate constants in the range of whole TiO_2 concentrations compared to the photocatalysis with mechanical stirring, though the rate constants decreased at more than 100 mg/L. The improvement can be evidenced by the higher enhancement factors (defined as the reaction rate of photocatalysis coupled with water jet cavitation divided by the rate of photocatalysis with stirring) of between 1.33 and 2.90. SEM photographs of the catalyst samples used in photocatalysis coupled with mechanical stirring and with water jet cavitation are shown in Fig. 6. The catalyst during photocatalytic treatment under mechanical stirring appear to be stuck together; however, separated nanoparticles can be observed in the SEM image of TiO_2 in the combined process of photocatalysis and water jet cavitation. This confirms the effect of particle deagglomeration induced by water jet cavitation. Overall, the photocatalysis coupled with water jet cavitation is more effective in degrading RR2 at lower TiO_2 concentrations than at higher TiO_2 concentrations.

3.4. Effect of RR2 concentration

The effect of initial amounts of RR2 on the dye decolorization was investigated with the RR2 concentrations ranging from 20 to 200 mg/L and TiO_2 loading of 100 mg/L using combined photocatalysis and water jet cavitation. Degradation efficiency of the

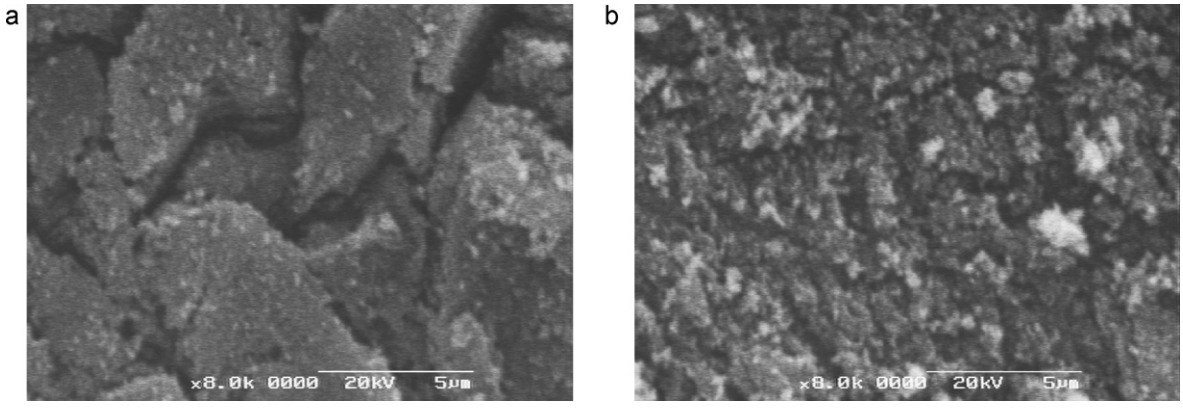

Fig. 6. SEM morphology of TiO_2 particles (a) after photocatalysis coupled with mechanical stirring for 90 min and (b) after photocatalysis coupled with water jet cavitation for 90 min.

Table 1
Degradation of RR2 by photocatalysis coupled with water jet cavitation at different dye concentration and solution pH (TiO_2 loading was 100 mg/L; Tube 1 was used as cavitation tube; no matrix component was added; treatment time was 90 min).

Initial RR2 concentration (mg/L)	Solution initial pH	Degradation efficiency in 90 min (%)	Rate constant $k \times 10^3$ (min^{-1})	R^2
20	6.7 (ambient)	98.8	40.9	0.9926
40	6.7	83.7	20.3	0.9994
80	6.7	60.5	10.4	0.9994
120	6.7	44.2	6.3	0.9958
200	6.7	28.8	3.7	0.9849
80	1.1	76.6	16.2	0.9996
80	3.2	70.5	13.7	0.9990
80	9.1	50.2	7.6	0.9974
80	11.2	32.4	4.2	0.9936

dye decreased with increasing initial concentration (Table 1). Over the treatment time of 90 min, the dye was degraded by up to 98.8% at the lowest RR2 concentration of 20 mg/L, compared to 28.8% at the highest concentration of 200 mg/L. Lower rate constant values shown in inset plot were progressively obtained with increasing initial concentration of RR2. The observation is consistent with the results of Mrowetz et al. [30], who observed a similar trend in the experiment using ultrasound to enhance the photocatalysis of an azo dye. As the initial concentrations of RR2 increased, the fraction of dye adsorbed on the catalyst and thereafter reacted with photogenerated holes or hydroxyl radicals decreased. Another possible reason is the progressively increasing filter effect of the dye within the solution [27].

It should be pointed out that the process efficiency in terms of absolute quantity of dye removal generally increased at higher initial concentrations though the degradation rate decreased with increasing initial concentration. For the initial concentration of 20, 40, 80, 120 and 200 mg/L, the amount of RR2 were removed by 19.8, 33.5, 48.4, 53.1 and 57.6 mg/L, respectively.

3.5. Effect of solution pH

pH is one of the important factors in determining the degradation rate and the process efficiency. The degradation efficiency of RR2 decreased with increase of pH value. As pH increased from 1.1 to 11.2, the dye decolorization was reduced from 76.6% to 32.4%, and the rate constant decreased from 16.2×10^{-3} to 4.2×10^{-3} min^{-1} (Table 1).

The effect of pH on the degradation rate can be related to the surface charge of TiO_2, the state of the dye molecule and the formation of hydroxyl radical. One RR2 molecule has two sulfonic groups ($-SO_3^-$) as water solubilizing group, which is negatively charged. When the pH was reduced to below 6.3, the isoelectric point of TiO_2 [31], the catalyst surface got positively charged, which favored the adsorption of the anionic dye. The adsorbed dye molecules may undergo hydroxyl radical attack, direct oxidation by positive holes and direct reduction by electrons [9]. As the pH value exceeds 6.3, the surface of TiO_2 gradually became more negatively charged, and the adsorption of the dye onto the TiO_2 surface was reduced, consequently inhibiting the dye degradation. It should be pointed out that the generation of hydroxyl radical was reported to be favored at high pH values [28]; however, this occurs via scavenging the photogenerated holes on the surface of TiO_2 particles through enough hydroxyl anions in alkaline media, which competes with the direct oxidative degradation of the dye by holes in valence band on TiO_2.

3.6. Effect of anions

Real industrial effluents commonly contain various inorganic anions such as SO_4^{2-}, Cl^-, NO_3^-, and HCO_3^- [32]. It is necessary to investigate the effects of the presence of these anions on the dye degradation. The unadjusted pH 6.7 was employed and the corresponding sodium salts were added individually with the concentration of 50 mM. NO_3^- and SO_4^{2-} increased RR2 removal, whereas the degradation efficiency was significantly reduced in presence of Cl^- or HCO_3^- (Fig. 7).

Zhu et al. [26] reported that the presence of NO_3^- evidently accelerated the photocatalytic degradation of an azo dye under visible light irradiation. The enhancement of degradation rate by NO_3^- may be mainly attribute to the direct or indirect formation of $^{\bullet}OH$ shown as follows [33],

$$NO_3^- + h\nu \rightarrow NO_2^- + O \quad (1)$$

$$NO_3^- + H_2O + h\nu \rightarrow NO_2^- + OH^- + {}^{\bullet}OH \quad (2)$$

$$O + H_2O \rightarrow 2{}^{\bullet}OH \quad (3)$$

The SO_4^{2-} played two roles in degradation of RR2. First, it increases the ionic strength of the aqueous phase, driving the dye molecule to the bulk-bubble interface and thus enhancing the cavitation efficiency [9]. Second, the adsorbed SO_4^{2-} reacts with photogenerated valence band holes to form $SO_4^{\bullet-}$ as follows [34]:

$$SO_4^{2-} + h_{VB}^+ \rightarrow SO_4^{\bullet-} \quad (4)$$

$$SO_4^{\bullet-} + H_2O \rightarrow SO_4^{2-} + {}^{\bullet}OH + H^+ \quad (5)$$

The generated $SO_4^{\bullet-}$ in Eq. (4) is a very strong oxidant with redox potential of +2.6 V and can participate in the degradation process [35]. Meanwhile, the reaction between SO_4^{2-} and h_{VB}^+ may inhibit the recombination of holes and electrons on the surface of photocatalyst, which consequently tends to enhance the degradation of

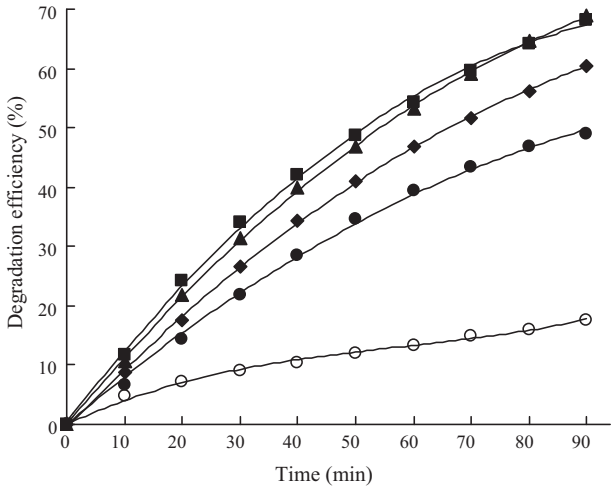

Fig. 7. Effect of anions on RR2 degradation during photocatalysis combined with water jet cavitation (initial pH was unadjusted; RR2 concentration was 80 mg/L; TiO_2 amount was 100 mg/L; Tube 1 was used as cavitation tube). -♦-, No matrix component; -■-, 50 mM $NaNO_3$; -▲-, 50 mM Na_2SO_4; -●-, 50 mM NaCl; -○-, 50 mM $NaHCO_3$.

RR2. This result was consistent with the previous findings on the degradation of monocrotophos [36] and 4-chlorophenol [37], but was contrary to some other reports [12,26]. The discrepancy could be attributed to the difference in the property of target contaminants and the solution–catalyst interface.

Addition of Cl^- had a detrimental effect on the degradation of the dye (Fig. 7). This can be explained by competitive adsorption or by the positive holes and hydroxyl radical scavenging properties of chloride ions [32]:

$$Cl^- + h_{VB}{}^+ \rightarrow Cl^\bullet \quad (6)$$

$$Cl^- + {}^\bullet OH \rightarrow Cl^\bullet + OH^- \quad (7)$$

The chloride radicals generated in Eqs. (6) and (7) have a lower oxidation potential of +2.47 V than hydroxyl radicals, which are with +2.80 V redox potential [38]. Therefore, the degradation rate of RR2 was considerably reduced by the presence of chloride ions.

When HCO_3^- was introduced to solution, a more pronounced negative effect than Cl^- on the decolorization was observed. The degradation efficiency of RR2 was decreased to 17.5% in the presence of 50 mM $NaHCO_3$. The negative effect of bicarbonate may be related to the pH shift from weak acidic to weak alkaline which inhibits dye degradation (Table 1). Moreover, the behavior of HCO_3^- is similar to Cl^- in that the HCO_3^- reacted with $^\bullet OH$ to form $CO_3^{-\bullet}$, less reactive than that of $^\bullet OH$ [18,39]. Thus, the degradation of RR2 was further suppressed.

4. Conclusions and implications

Coupling photocatalysis with water jet cavitation enhanced the RR2 degradation efficiency and showed a synergistic effect, compared to individual photocatalysis or water jet cavitation. This may be attributed to the elevated catalytic activity of TiO_2 and increased production of reactive free radicals by the jet cavitation process.

The combined process is more effective in degrading RR2 at lower TiO_2 concentrations than at higher TiO_2 concentrations. Venturi tube with smaller diameter and shorter length of throat tube is preferred for the dye decolorization. The RR2 degradation followed pseudo-first-order reaction and the degradation rate constant increased with the decreasing initial dye concentration and solution pH. The presence of NO_3^- and SO_4^{2-} enhanced the degradation of RR2, while addition of Cl^-, and especially HCO_3^- ions had an inhibitory effect on the dye decolorization.

As a novel AOPs, water jet cavitation possesses the advantages of lower cost and higher energy efficiency, and it is more suitable for large-scale application compared with acoustic cavitation [24]. In this study, the combined treatment of photocatalysis and water jet cavitation showed a significant enhancement of photocatalytic efficiency on the RR2 degradation in a large volume of 4.0 L solution. This suggests a possibility of photocatalytic chemistry coupled with water jet cavitation for wastewater treatment at a practical full scale; and to achieve an adequate reaction rate, the use of water jet cavitation on photocatalytic process can significantly reduce the dose of photocatalyst, which is more economical and environment-friendly, especially for large-scale application.

Acknowledgments

This work was partly supported by National Natural Science Foundation of China (No. 50878126). The authors gratefully acknowledge Professor Xinde Cao for helpful discussion.

References

[1] R. Vinu, G. Madras, Kinetics of sonophotocatalytic degradation of anionic dyes with nano-TiO_2, Environ. Sci. Technol. 43 (2009) 473–479.
[2] J.C. Garcia, J.L. Oliveira, A.E.C. Silva, C.C. Oliveira, J. Nozaki, N.E. de Souza, Comparative study of the degradation of real textile effluents by photocatalytic reactions involving UV/TiO_2/H_2O_2 and UV/Fe^{2+}/H_2O_2 systems, J. Hazard. Mater. 147 (2007) 105–110.
[3] H. Zollinger, Color Chemistry: Synthesis, Properties and Applications of Organic Dyes and Pigments, VCH Publishers, New York, 1987.
[4] D.E. Kritikos, N.P. Xekoukoulotakis, E. Psillakis, D. Mantzavinos, Photocatalytic degradation of reactive black 5 in aqueous solutions: Effect of operating conditions and coupling with ultrasound irradiation, Water Res. 41 (2007) 2236–2246.
[5] H.-J. Hsing, P.-C. Chiang, E.-E. Chang, M.-Y. Chen, The decolorization and mineralization of Acid Orange 6 azo dye in aqueous solution by advanced oxidation processes: a comparative study, J. Hazard. Mater. 141 (2007) 8–16.
[6] A. Mohey El-Dein, J.A. Libra, U. Wiesmann, Mechanism and kinetic model for the decolorization of the azo dye Reactive Black 5 by hydrogen peroxide and UV radiation, Chemosphere 52 (2003) 1069–1077.
[7] I.K. Konstantinou, T.A. Albanis, TiO_2-assisted photocatalytic degradation of azo dyes in aqueous solution: Kinetic and mechanistic investigations: a review, Appl. Catal. B: Environ. 49 (2004) 1–14.
[8] P.R. Gogate, Treatment of wastewater streams containing phenolic compounds using hybrid techniques based on cavitation: a review of the current status and the way forward, Ultrason. Sonochem. 15 (2008) 1–15.
[9] C.-H. Wu, Effects of sonication on decolorization of C.I. Reactive Red 198 in UV/ZnO system, J. Hazard. Mater. 153 (2008) 1254–1261.
[10] C.G. Joseph, G. Li Puma, A. Bono, D. Krishnaiah, Sonophotocatalysis in advanced oxidation process: a short review, Ultrason. Sonochem. 16 (2009) 583–589.
[11] Y.-C. Chen, P. Smirniotis, Enhancement of photocatalytic degradation of phenol and chlorophenols by ultrasound, Ind. Eng. Chem. Res. 41 (2002) 5958–5965.
[12] L.H. Thompson, L.K. Doraiswamy, Sonochemistry: science and engineering, Ind. Eng. Chem. Res. 38 (1999) 1215–1249.
[13] K.S. Suslick, Ultrasound: Its Chemical, Physical and Biological Effects, VCH Publishers, New York, 1988.
[14] K.M. Kalumuck, G.L. Chahine, The use of cavitating jets to oxidize organic compounds in water, J. Fluids Eng. Trans. ASME 122 (2000) 465–470.
[15] G.V. Ambulgekar, S.D. Samant, A.B. Pandit, Oxidation of alkylarenes to the corresponding acids using aqueous potassium permanganate by hydrodynamic cavitation, Ultrason. Sonochem. 11 (2004) 191–196.
[16] P.R. Gogate, Cavitation:, An auxiliary technique in wastewater treatment schemes, Adv. Environ. Res. 6 (2002) 335–358.
[17] A.G. Chakinala, D.H. Bremner, P.R. Gogate, K.-C. Namkung, A.E. Burgess, Multivariate analysis of phenol mineralisation by combined hydrodynamic cavitation and heterogeneous advanced Fenton processing, Appl. Catal. B: Environ. 78 (2008) 11–18.
[18] X. Wang, J. Jia, Y. Wang, Electrochemical degradation of reactive dye in the presence of water jet cavitation, Ultrason. Sonochem. 17 (2010) 515–520.
[19] P. Senthil Kumar, M. Siva Kumar, A.B. Pandit, Experimental quantification of chemical effects of hydrodynamic cavitation, Chem. Eng. Sci. 55 (2000) 1633–1639.
[20] K.S. Suslick, M.M. Mdleleni, J.T. Ries, Chemistry induced by hydrodynamic cavitation, J. Am. Chem. Soc. 119 (1997) 9303–9304.
[21] N.L. Stock, J. Peller, K. Vinodgopal, P.V. Kamat, Combinative sonolysis and photocatalysis for textile dye degradation, Environ. Sci. Technol. 34 (2000) 1747–1750.
[22] W. Feng, D. Nansheng, H. Helin, Degradation mechanism of azo dye C.I. reactive red 2 by iron powder reduction and photooxidation in aqueous solutions, Chemosphere 41 (2000) 1233–1238.
[23] N.P. Vichare, P.R. Gogate, A.B. Pandit, Optimization of hydrodynamic cavitation using a model reaction, Chem. Eng. Technol. 23 (2000) 683–690.
[24] M. Sivakumar, A.B. Pandit, Wastewater treatment: a novel energy efficient hydrodynamic cavitational technique, Ultrason. Sonochem. 9 (2002) 123–131.
[25] P.R. Gogate, A.B. Pandit, Engineering design methods for cavitation reactors II: Hydrodynamic cavitation, AIChE J. 46 (2000) 1641–1649.
[26] H. Zhu, R. Jiang, L. Xiao, Y. Chang, Y. Guan, X. Li, G. Zeng, Photocatalytic decolorization and degradation of Congo Red on innovative crosslinked chitosan/nano-CdS composite catalyst under visible light irradiation, J. Hazard. Mater. 169 (2009) 933–940.
[27] E. Selli, Synergistic effects of sonolysis combined with photocatalysis in the degradation of an azo dye, Phys. Chem. Chem. Phys. 4 (2002) 6123–6128.
[28] J. Wang, T. Ma, Z. Zhang, X. Zhang, Y. Jiang, D. Dong, P. Zhang, Y. Li, Investigation on the sonocatalytic degradation of parathion in the presence of nanometer rutile titanium dioxide (TiO_2) catalyst, J. Hazard. Mater. 137 (2006) 972–980.
[29] L. Davydov, E.P. Reddy, P. France, P.G. Smirniotis, Sonophotocatalytic destruction of organic contaminants in aqueous systems on TiO_2 powders, Appl. Catal. B: Environ. 32 (2001) 95–105.
[30] M. Mrowetz, C. Pirola, E. Selli, Degradation of organic water pollutants through sonophotocatalysis in the presence of TiO_2, Ultrason. Sonochem. 10 (2003) 247–254.
[31] M.R. Hoffmann, S.T. Martin, W. Choi, D.W. Bahnemann, Environmental applications of semiconductor photocatalysis, Chem. Rev. 95 (1995) 69–96.
[32] H.-c. Liang, X.-z. Li, Y.-h. Yang, K.-h. Sze, Effects of dissolved oxygen, pH, and anions on the 2,3-dichlorophenol degradation by photocatalytic reaction with anodic TiO_2 nanotube films, Chemosphere 73 (2008) 805–812.
[33] R.G Zepp, J. Hoigneĭ, H. Bader, Nitrate-induced photooxidation of trace organic chemicals in water, Environ. Sci. Technol. 21 (1987) 443–450.

[34] L. Ravichandran, K. Selvam, M. Swaminathan, Effect of oxidants and metal ions on photodefluoridation of pentafluorobenzoic acid with ZnO, Sep. Purif. Technol. 56 (2007) 192–198.
[35] Y.G. Adewu-Yi, Sonochemistry in environmental remediation. 2. Heterogeneous sonophotocatalytic oxidation processes for the treatment of pollutants in water, Environ. Sci. Technol. 39 (2005) 8557–8570.
[36] Z. Hua, Z. Manping, X. Zongfeng, G.K.-C. Low, Titanium dioxide mediated photocatalytic degradation of monocrotophos, Water Res. 29 (1995) 2681–2688.
[37] U.I. Gaya, A.H. Abdullah, Z. Zainal, M.Z. Hussein, Photocatalytic treatment of 4-chlorophenol in aqueous ZnO suspensions: Intermediates, influence of dosage and inorganic anions, J. Hazard. Mater. 168 (2009) 57–63.
[38] C.-S. Lu, C.-C. Chen, F.-D. Mai, H.-K. Li, Identification of the degradation pathways of alkanolamines with TiO_2 photocatalysis, J. Hazard. Mater. 165 (2009) 306–316.
[39] D. Mijin, M. Savić, P. Snežana, A. Smiljanić, O. Glavaški, M. Jovanović, S. Petrović, A study of the photocatalytic degradation of metamitron in ZnO water suspensions, Desalination 249 (2009) 286–292.